Inorganic Chemistry
Article

Inorg. Chem. **2010**, *49*, 2983–2989 **2983**
DOI: 10.1021/ic902490z

Reactions of Organyl and Silyl Alanes with 1,3,4,5,6-Pentamethyl-2-aminoborazine

Maomin Fan,[†] Eileen N. Duesler,[†] Heinrich Nöth,[‡] and Robert T. Paine*[,†]

[†]*Department of Chemistry, University of New Mexico, Albuquerque, New Mexico 87131, and* [‡]*Department of Chemistry, University of Munich, Butenandstrasse 5-13, 81377, Munich, Germany*

Received December 15, 2009

The reactions of $(Me_3Si)_3Al$, Me_3Al, Et_3Al, and *i*-Bu_3Al with 1,3,4,5,6-pentamethyl-2-aminoborazine have been examined. An amine alane adduct $(Me_3Si)_3Al\cdot NH_2B_3(Me)_2N_3Me_3$ (**1**) and several elimination products $[(Me_3Si)_2AlN(H)B_3(Me)_2N_3Me_3]_2$ (**2**), $[(Me_3SiAl)_4(Me_3SiN)_3NH]$ (**3**), $[Me_2AlN(H)\ B_3(Me)_2N_3Me_3]_2$ (**4**), $[Et_2AlN(H)\ B_3(Me)_2N_3Me_3]_2$ (**5**), and $[i\text{-}Bu_2AlN(H)\ B_3(Me)_2N_3Me_3]_2$ (**6**) have been isolated. Compounds **1**, **2**, **4**−**6** have been spectroscopically characterized, and single crystal X-ray diffraction structure determinations have been completed for **1**−**4** and **6**. The molecular chemistry provides insight into the reaction of Me_3Al and 1,3,5-*N*-trimethyl-2,4,6-*B*-triaminoborazine that, upon pyrolysis, produces AlN/BN composite ceramic materials.

Introduction

Many coordination compounds of the general type $X_3Al\cdot NY_3$ are known[1−3] and in the case of tertiary organyl amines, these adducts are thermodynamically stable. However, it is also known that alkyl alanes, R_3Al, in combination with NH_3, primary and secondary amines, provide competing R-H elimination pathways. Typically these lead to formation of amino alane, $R_2Al\text{-}NY_2$, and imino alane, $RAl\text{-}NY$, species most of which, in the absence of steric protection, condense producing a diverse array of structurally interesting products.[1−10] In the past, we[11] and others[12] have examined several of these combinations as molecular precursors for the important binary ceramic AlN as well as for mixed binary phase compositions, for example, TiN/BN,[13] ZrN/BN, AlN/SiC,[10b] and ternary materials, for example $Ti_xB_yN_z$,[13] $Si_xB_yN_z$,[11b] and $Si_xAl_yN_z$.[14] We describe here the results from a study of reactions of organyl and silyl alanes with 1,3,4,5,6-pentamethyl-2-aminoborazine as models for reactions of Me_3Al with borazinylamines that lead to the formation of solid-state materials containing nanodispersed crystalline AlN in a BN matrix.

*To whom correspondence should be addressed. E-mail: rtpaine@unm.edu.

(1) Mole, T.; Jeffery, E. A. *Organoaluminum Chemistry*; Elsevier: New York, 1972; pp 229−249.
(2) Bradley, D. C. *Adv. Inorg. Chem. Radiochem.* **1972**, *15*, 259.
(3) Schulz, S. *Adv. Organomet. Chem.* **2003**, *49*, 225–317.
(4) Bahr, G. In *Inorganic Chemistry, part II; FIAT Review of WWII German Science*; Klemm, W., Ed.; Dieterichsche Verlagsbuchhandlung: Wiesbaden, Germany, 1948; Vol. *24*.
(5) Lappert, M. F.; Power, P. P.; Sangar, A. R.; Srivastava, R. C. *Metal and Metalloid Amides − Synthesis, Structures and Physical and Chemical Properties*; Wiley: New York, 1980; pp 99−117.
(6) *Chemistry of Aluminum, Gallium, Indium and Thallium*; Downs, A. J., Ed.; Chapman and Hall: London, 1993.
(7) Cesari, M.; Cucinella, S. In *The Chemistry of Inorganic Homo- and Heterocycles*; Haiduc, I., Sowerby, D. B., Eds.; Academic Press: London, 1987; Vol. *1*.
(8) Veith, M. *Chem. Rev.* **1990**, *90*, 3–16.
(9) Timoshkin, A. Y. *Coord. Chem. Rev.* **2005**, *249*, 2094–2131.
(10) (a) Waggoner, K. M.; Power, P. P. *J. Am. Chem. Soc.* **1991**, *113*, 3385–3393. (b) Davidson, M. G.; Elilio, D.; Less, S .L.; Martin, A.; Raithley, R. R.; Snaith, R.; Wright, D. S. *Organometallics* **1993**, *12*, 1–3. (c) Schaur, S. J.; Pennington, W. T.; Robinson, G. H. *Organometallics* **1992**, *11*, 3287–3292. (d) Belgardt, T.; Waezsada, S. D.; Roesky, H. W.; Gornitzka, H.; Häming, L.; Stalke, D. *Inorg. Chem.* **1994**, *33*, 6247–6251. (e) Bradley, D. C.; Harding, I. S.; Maia, I. A.; Motevalli, M. *J. Chem., Soc. Dalton Trans.* **1997**, 2969–2979. (f) Fischer, R. A.; Weiss, J. *Angew. Chem., Int. Ed.* **1999**, *38*, 2830–2850. (g) Dureen, M. A.; Stephan, D. W. *Dalton Trans.* **2008**, 4723–4731 and references therein.
(11) (a) Janik, J. F.; Duesler, E. N.; Paine, R. T. *Inorg. Chem.* **1987**, *26*, 4341–4345. (b) Janik, J. F.; Duesler, E. N.; Paine, R. T. *Inorg. Chem.* **1988**, *27*, 4335–4338. (c) Paine, R. T.; Janik, J. F.; Narula, C. K. *Mater. Res. Soc. Symp. Proc.* **1988**, *121*, 461–464. (d) Janik, J. F.; Paine, R. T. *J. Organomet. Chem.* **1993**, *449*, 39–44. (e) Janik, J. F.; Duesler, E. N.; Paine, R. T. *Chem. Ber.* **1993**, *126*, 2649–2651. (f) Bartram, M. E.; Michalski, T. A.; Rogers, J. W., Jr.; Paine, R. T. *Chem. Mater.* **1993**, *5*, 1424–1430. (g) Janik, J. F.; Duesler, E. N.; Paine, R. T. *J. Organomet. Chem.* **1997**, *539*, 19–25.
(12) (a) Interrante, L. V.; Carpenter, L., Jr.; Whitmarsh, C.; Lee, W.; Garbouskas, M.; Slack, G .A. *Mater. Res. Soc. Symp. Proc.* **1986**, *73*, 359–366. (b) Seibold, M. M.; Rüssel, C. *Mater. Res. Soc. Symp. Proc.* **1988**, *121*, 477–482. (c) Baker, R. T.; Bolt, J. D.; Reddy, G. S.; Roe, D. C.; Staley, R. H.; Tebbe, F. N.; Vega, A. J. *Mater. Res. Soc. Symp. Proc.* **1988**, *121*, 471–476. (d) Seibold, M. M.; Rüssel, C. *J. Am. Ceram. Soc.* **1989**, *72*, 1503–1505. (e) Gladfelter, W. L.; Boyd, D. C.; Jensen, K. F. *Chem. Mater.* **1989**, *1*, 339–343. (f) Interrante, L. V.; Sigel, G.; Garbouskas, M.; Hejna, C. *Phosphorus, Sulfur and Silicon* **1989**, *41*, 325–334. (g) Interrante, L. V.; Sigel, G. A.; Garbouskas, M.; Hejna, C.; Slack, G. A. *Inorg. Chem.* **1989**, *28*, 252–257. (h) Sauls, F. C.; Interrante, L. V.; Jiang, Z. *Inorg. Chem.* **1990**, *29*, 2989–2996. (i) Jiang, Z.; Interrante, L. V. *Chem. Mater.* **1990**, *2*, 439–446. (j) Jiang, Z.; Interrante, L. V.; Kwon, D.; Tham, F. S.; Kullnig, R. *Inorg. Chem.* **1991**, *30*, 995–1000. (k) Bartram, M. E.; Michalski, T. A.; Rogers, J. W., Jr.; Mayer, T. M. *Chem. Mater.* **1991**, *3*, 953–960. (l) Sauls, F. C.; Interrante, L. V. *Coord. Chem. Rev.* **1993**, *128*, 193–207. (m) Paciorek, K. J. L.; Nakahara, J. H.; Hoferkamp, L. A.; George, C.; Flippen-Anderson, J. L.; Gilardi, R.; Schmidt, W. R. *Chem. Mater.* **1991**, *3*, 82–87.
(13) Fan, M.; Duesler, E. N.; Janik, J. F.; Paine, R. T. *J. Inorg. Organomet. Polym. Mater.* **2007**, *17*, 423–437.
(14) Srivastava, D.; Fan, M.; Duesler, E. N.; Paine, R. T. *Eur. J. Inorg. Chem.* **1998**, 855–859.

Published on Web 02/16/2010

Experimental Section

General Information. Inert atmosphere methods were used for the handling of all reagents, and solvents were rigorously dried and stored protected by dry nitrogen. Infrared spectra were recorded on a Nicolet 6000 FT-IR spectrometer from KBr pellets. Mass spectra were obtained with a Finnegan 4500 mass spectrometer by using a solids inlet probe. NMR spectra were recorded on Bruker AC-250 and JEOL-400 spectrometers. Spectral standards were Me_4Si (^1H, ^{13}C) and $F_3B\cdot OEt_2$ (^{11}B). The $(Me_3Si)_3Al\cdot OEt_2$ complex was prepared as described in the literature[15] and Me_3Al, Et_3Al, and *i*-Bu_3Al were purchased from Aldrich. The 1,3,4,5,6-pentamethyl-2-aminoborazine (**PMAB**) was prepared as described previously.[16]

Reaction of $(Me_3Si)_3Al\cdot OEt_2$ and PMAB. A sample of **PMAB** (0.52 g, 3.1 mmol) in hexane (15 mL) was combined while stirring with $(Me_3Si)_3Al\cdot OEt_2$ (1.0 g, 3.1 mmol) in hexane (20 mL) at −78 °C. After 4 h at −78 °C, the mixture was warmed (23 °C) and stirred (15 h). Volatiles were removed by vacuum evaporation leaving a white solid, $(Me_3Si)_3Al\cdot$PMAB (**1**). Yield: 1.1 g (89%). The solid was recrystallized from hexane providing colorless single crystals: mp 95−97 °C (decomp). Mass spectrum (EI, 30 eV, *m*/*z*): 412 (M^+). Infrared spectrum (KBr, cm^{-1}): 3360 (w), 3308 (w), 2942 (s), 2890 (s), 2832 (m), 1609 (m), 1559 (m), 1474 (vs), 1449 (vs), 1404 (br, vs), 1281 (m), 1246 (s), 1109 (s), 1051 (m), 1028 (m), 963 (s), 835 (vs), 762 (w), 719 (w), 611 (m). ^1H NMR (C_6D_6): δ 0.28 (s, Si*Me*, 27H), 0.39 (s, B-4,6 *Me*, 6H), 1.89 (s, N*H*$_2$, 2H), 2.53 (s, N-1,3 *Me*, 6H), 2.62 (s, N-5 *Me*, 3H). $^{13}C\{^1H\}$ NMR (C_6D_6): δ - 0.02 (B-4,6 *Me*), 2.88 (Si*Me*), 32.60 (N-1,3 *Me*), 34.68 (N-5 *Me*). $^{11}B\{^1H\}$ NMR (C_6D_6): δ 27.29 (*B*-2), 37.59 (*B*4,6). Anal. Calcd for $C_{11}H_{34}AlB_3N_4Si_3$: C, 40.79; H, 10.76; N, 13.59. Found: C, 40.57; H, 10.65; N, 13.04.

Decomposition of $(Me_3Si)_3Al\cdot$PMAB. A sample of $(Me_3Si)_3Al\cdot OEt_2$ (1.0 g, 3.1 mmol) in hexane (20 mL) was added to a solution of **PMAB** (0.52 g, 3.1 mmol) in hexane (20 mL) at −78 °C. The mixture was warmed to 23 °C and stirred (12 h). The volatiles were vacuum evaporated, the residue (**1**) redissolved in toluene (30 mL), and the solution refluxed (24 h). Volatiles were vacuum evaporated, and the solid residue washed with hexane (2 × 10 mL) leaving a white solid $[(Me_3Si)_2AlN(H)Me_2B_3N_3Me_3]_2$ (**2**). Yield: 0.90 g, 85%. The solid was recrystallized from hot hexane providing colorless single crystals: mp 190−192 °C (decomp.). Mass spectrum (EI, 30 eV, *m*/*z*): 661 ($M - Me^+$). Infrared spectrum (KBr, cm^{-1}): 3264 (w), 2949 (m), 2893 (s), 2834 (m), 1605 (w), 1456 (br, s), 1404 (br, s), 1283 (m), 1250 (s), 1198 (m), 1103 (s), 1036 (m), 882 (m), 837 (vs), 764 (m), 677 (m). *Cis* isomer: ^1H NMR (C_6D_6): δ 0.20 (s, Si*Me*, 18H), 0.33 (s, Si*Me*, 18H), 0.43 (s, B-4,6 *Me*, 12H), 2.65 (s, N-5 *Me*, 6H), 3.14 (s, N-1,3 *Me*, 12H), 3.55 (br, N*H*, 2H). $^{13}C\{^1H\}$ NMR (C_6D_6): δ 1.73 (*Me*$_3$Si), 2.07 (*Me*$_3$Si), 34.46 (N-5 *Me*), 35.63 (N-1, 3 *Me*). *Trans* isomer: ^1H NMR (C_6D_6): δ 0.28 (s, Si*Me*, 36H), 0.42 (s, B-4,6 *Me*, 12H), 2.63 (s, N-5 *Me*, 6H), 3.15 (s, N-1,3 *Me*, 12H), 3.63 (br, N*H*, 2H). $^{13}C\{^1H\}$ (C_6D_6): δ 1.82 (*Me*$_3$Si), 34.48 (N-5 *Me*), 35.75 (N-1,3 *Me*). *Cis*/*Trans* 1/2.8. $^{11}B\{^1H\}$ NMR (C_6D_6): δ 26.1 (*B*2), 36.1 (*B*4,6). Anal. Calcd. for $C_{22}H_{68}Al_2B_6N_8Si_4$: C, 39.09; H, 10.14; N, 16.58. Found: C, 38.64; H, 11.11; N, 15.39. Trap to trap vacuum separation of the reaction volatiles led to identification of Me_3SiH as the byproduct.

Formation of $[(Me_3SiAl)_4(Me_3SiN)_3NH]$ (3). A sample of **2** (0.4 g, 0.6 mmol) was dissolved in toluene (20 mL) and refluxed (3 d). Volatiles were vacuum evaporated and the white solid residue washed with hexane (3 × 10 mL) leaving a white solid. ^1H NMR analysis indicated that the majority of the sample remained as **2**; however, several low intensity resonances (δ 0.35, 0.46) suggested the presence of a second component (∼20%). Recrystallization from hot hexane/toluene mixture gave crystalline samples containing **2** and **3**. The more blocky morphology crystals were identified by single crystal X-ray diffraction analysis as **3**.

Reaction of Me_3Al with PMAB. A sample of Me_3Al (5 mL, 2.0 M solution in toluene, 10 mmol) was added dropwise to a solution of **PMAB** (1.7 g, 10 mmol) in toluene (30 mL) at 23 °C. The reaction mixture was stirred (15 h) and evolved CH_4 was collected and identified by IR spectroscopy. Solvent was evaporated leaving a white residue. Recrystallization from hexane produced colorless crystalline $[Me_2AlN(H)Me_2B_3N_3Me_3]_2$ (**4**). Yield: 2.0 g (90%), mp 184-186 °C (decomp). Mass spectrum (EI, 30 eV, *m*/*z*): 428 ($M\text{-}CH_3^+$). Infrared spectrum (KBr, cm^{-1}): 3273 (w), 3027 (w), 2938 (m), 2922 (m), 2826 (w), 1481 (vs), 1456 (vs), 1389 (br, vs), 1339 (s), 1298 (m), 1219 (s), 1198 (s), 1101 (s), 1034 (m), 1009 (vw), 882 (m), 866 (s), 772 (m), 702 (s), 685 (s), 586 (m). *Cis* isomer: ^1H NMR (C_6D_6): δ −0.33 (s, Al*Me*, 6H), −0.24 (s, Al*Me*, 6H), 0.41 (s, B-4,6 *Me*, 12H), 2.69 (s, N-5 *Me*, 6H), 2.90 (s, N-1,3 *Me*, 12H). $^{13}C\{^1H\}$ (C_6D_6): δ −5.28 (Al*Me*), 0.11 (B-4,6 *Me*), 34.55 (N-5 *Me*), 34.61 (N-1,3 *Me*). *Trans* isomer: ^1H NMR (C_6D_6): δ −0.28 (s, Al*Me*, 12H), 0.41 (s, B-4,6 *Me*, 12H), 2.68 (s, N-5 *Me*, 6H), 2.87 (s, N-1,3 *Me*, 12H) *Cis*/*Trans* 1/1.6. $^{11}B\{^1H\}$ NMR (C_6D_6): δ 28.7 (*B*2), 37.2 (*B*4,6). Anal. Calcd for $C_{14}H_{44}B_6N_8Al_2$: C, 37.93; H, 10.00; N, 25.27. Found: 37.77; H, 9.81; N, 23.98.

Reaction of Et_3Al with PMAB. A sample of Et_3Al (4 mL, 1.90 M in toluene, 7.6 mmol) was added with stirring to **PMAB** (1.3 g, 7.6 mmol) in toluene (30 mL) at 23 °C. The mixture was stirred (20 h) and then refluxed (2 h). Ethane was detected in the off-gas by IR and solvent was removed by vacuum evaporation. The resulting white residue was recrystallized from hexane forming colorless crystals of $[Et_2AlN(H)Me_2B_3N_3Me_3]_2$ (**5**). Yield: 1.3 g (71%), mp 171−173 °C. Mass spectrum (EI, 30 eV, *m*/*z*): 499 (M^+). Infrared spectrum (KBr, cm^{-1}): 3268 (m), 2938 (s), 2903 (s), 2863 (s), 1603 (m), 1479 (vs), 1456 (vs), 1398 (br, vs), 1292 (m), 1215 (s), 1101 (s), 1034 (m), 984 (m), 953 (m), 882 (s), 856 (s), 770 (m), 696 (s), 665 (s), 619 (s), 557 (m), 536 (m). *Cis* isomer. ^1H NMR (C_6D_6): δ 0.41−0.56 (s, br, AlC*H*$_2$, 8H), 1.13−1.37 (s, br, AlCH$_2$C*H*$_3$, 12H), 0.43 (s, B-4,6 *Me*, 12H), 2.67 (s, N-5 *Me*, 6H), 2.92 (s, N-1,3 *Me*, 12H). $^{13}C\{^1H\}$ (C_6D_6): δ 0.16 (B-4,6 *Me*), 3.09 (Al*C*H$_2$), 8.65 (AlCH$_2$*C*H$_3$), 9.52 (AlCH$_2$*C*H$_3$), 34.41 (N-5 *Me*), 34.54 (N-1,3 *Me*). *Trans* isomer. ^1H (C_6D_6): δ 0.25−0.41 (s, br, AlC*H*$_2$, 8H), 1.13−1.37 (s, br, AlCH$_2$C*H*$_3$, 12H), 0.43 (s, B-4,6 *Me*, 12H), 2.68 (s, N-5 *Me*, 6H), 2.96 (s, N-1, 3 *Me*, 12H). $^{13}C\{^1H\}$ (C_6D_6): δ 0.16 (B-4,6 *Me*), 3.71 (Al*C*H$_2$), 9.04 (AlCH$_2$*C*H$_3$), 34.41 (N-5 *Me*), 34.54 (N-1,3 *Me*) *Cis*/*Trans* 1/1.1. $^{11}B\{^1H\}$ (C_6D_6): δ 29.3 (*B*2), 37.5 (*B*4,6). Anal. Calcd. $C_{18}H_{52}Al_2B_6N_4$: C, 43.28; H, 10.49; N, 22.43. Found: C, 43.42; H, 11.21; N, 20.43.

Reaction of *i*-Bu_3Al with PMAB. A sample of *i*-Bu_3Al (10 mL, 1.0 M in toluene, 10 mmol) was added to a solution of **PMAB** (1.7 g, 10 mmol) in toluene (20 mL) at 23 °C, which was stirred (23 °C, 2 h) and then refluxed (4 h). Volatiles were removed by vacuum evaporation, and the white residue was recrystallized from hexane leaving single crystals of $[i\text{-}Bu_2AlN(H)Me_2B_3N_3Me_3]_2\cdot[Me_3N_3B_3(Me)_2(NH_2)]_{0.5}$, ($\mathbf{6}\cdot[Me_3N_3B_3(Me)_2(NH_2)]_{0.5}$). Yield: 2.0 g (65%), mp 108−110 °C. Mass spectrum (EI, 30 eV, *m*/*z*): 555 ($M\text{-}(CH_3)_2CHCH_2^+$). Infrared spectrum (KBr, cm^{-1}): 3273 (w), 2949 (vs), 2863 (s), 2783 (w), 1605 (m), 1454 (br, vs), 1406 (br, vs), 1289 (m), 1250 (m), 1217 (m), 1198 (m), 1101 (s), 1065 (m), 1036 (m), 1013 (w), 880 (m), 856 (m), 814 (w), 770 (w), 647 (m), 484 (m). *Cis* isomer. ^1H NMR (C_6D_6): δ 0.30−0.62 (m, AlC*H*$_2$), 0.45 (s, B-4,6 *Me*), 1.01 (d, C*H*$_3$, J_{HH} = 6.5 Hz, 24H), 1.15 (d, C*H*$_3$, J_{HH} = 6.4 Hz, 24H), 2.08 (m, C*H*), 2.66 (s, N-5 *Me*, 6 H), 3.03 (s, N-1,3 Me, 12H). *Trans* isomer. ^1H NMR (C_6D_6): δ 0.30−0.61 (m, AlC*H*$_2$), 0.45 (s, B-4,6 *Me*), 1.09 (d, C*H*$_3$, J_{HH} = 6.4 Hz, 24H), 2.08 (m, C*H*), 2.65 (s, N-5 *Me*, 6 H), 3.01 (s, N-1, 3 *Me*, 12H).

(15) (a) Rösch, L. *Angew. Chem., Int. Ed. Engl.* **1977**, *16*, 480. (b) Rösch, L.; Altnau, G. *J. Organomet. Chem.* **1980**, *195*, 47–53.

(16) (a) Narula, C. K.; Lindquist, D. A.; Fan, M.; Borek, T. T.; Duesler, E. N.; Datye, A. K.; Schaeffer, R.; Paine, R. T. *Chem. Mater.* **1990**, *2*, 377–384. (b) Toeniskoetter, R. H.; Hall, F. R. *Inorg. Chem.* **1963**, *2*, 29–36.

Table 1. Crystallographic Data for $1\cdot(Me_3B_3N_3Me_3)_{0.5}$, **2**, **3**, **4**, and $6\cdot[Me_3N_3B_3(Me)_2(NH_2)]_{0.5}$

	$1\cdot(Me_3B_3N_3Me_3)_{0.5}$	**2**	**3**	**4**	$6\cdot[Me_3N_3B_3(Me)_2(NH_2)]_{0.5}$
compound code	MF09A	MF14	MF10	MF13	MF04
empirical formula	$C_{17}H_{53}AlB_{4.5}N_{5.5}Si_3$	$C_{11}H_{34}AlB_3N_4Si_2$	$C_{21}H_{64}Al_4N_4Si_7$	$C_7H_{22}AlB_3N_4$	$C_{15.5}H_{42.5}AlB_{4.5}N_6$
formula weight	494.5	338.0	677.3	221.7	388.7
cryst syst	monoclinic	monoclinic	orthorhombic	triclinic	monoclinic
space group	$P2(1)/n$	$C2/c$	$Cmc2(1)$	$P\bar{1}$	$P2(1)/c$
a (Å)	9.923(3)	23.60(1)	18.375(6)	7.600(1)	12.276(3)
b (Å)	19.379(5)	10.218(4)	18.713(8)	8.254(1)	11.766(3)
c (Å)	17.281(5)	19.141(9)	12.815(5)	11.416(2)	17.499(5)
α (deg)	90	90	90	92.93(1)	90
β (deg)	92.15(2)	107.36(6)	90	98.83(1)	90.30(2)
γ (deg)	90	90	90	107.02(1)	90
V (Å^3)	3320.6(2)	4406(3)	4407(3)	673.2(2)	2527(1)
Z	4	8	4	2	4
T (K)	298	293	293	293	293
D_{calcd} (g cm^{-3})	0.989	1.019	1.021	1.094	1.021
μ (MoKα)(mm^{-1})	0.179	0.194	0.306	0.121	0.088
independent data	5841	3278	2112	2363	4480
observed data ($F > n\sigma(F)$)	2723(2.5$\sigma(F)$)	2233(3$\sigma(F)$)	1367(2.5$\sigma(F)$)	1561(3$\sigma(F)$)	2152(3$\sigma(F)$)
parameters	286	193	182	140	217
R1[a]	0.0924	0.0819	0.0756	0.0651	0.0978
wR2[b] (all data)	0.0792	0.0796	0.1210	0.0806	0.1055

[a] $R1 = \sum||F_o| - |F_c||/\sum|F_o|$. [b] $wR2 = \{\sum w(F_o^2 - F_c^2)^2/\sum w(F_o^2)^2\}^{1/2}$.

$^{12}C\{^1H\}$ (C_6D_6): δ 0.14 (B*Me*), 26.51, 26.76, 27.12 (*C*H$_2$), 28.12, 28.71 (*C*H), 28.21, 28.55 (*C*H$_3$), 34.51, 35.27 (N*Me*) *Cis*/*Trans* 2/1. $^{11}B\{^1H\}$ (C_6D_6): δ 25.8 (*B*2), 35.9 (*B*4,6). Anal. Calcd. for $C_{31}H_{85}Al_2B_9N_{12}$: C, 47.90; H, 11.02; N, 21.62. Found: C, 48.39; H, 11.26; N, 19.02.

Pre-ceramic Precursor Synthesis and Pyrolysis. A sample of Me_3Al (10 mL, 2.0 M in toluene, 20 mmol) was combined with $(MeNBNH_2)_3$ (**7**) (1.12 g, 6.7 mmol) in toluene (30 mL) at 23 °C. The mixture was stirred at 23 °C (45 h) and refluxed (1 h). Methane was evolved during the reaction, and this was trapped and identified by its gas phase IR spectrum. The solvent was vacuum evaporated leaving a glassy solid (**8**) that was soluble in toluene and benzene but not in liquid NH_3 at 0 °C. Yield 2.0 g (90% based on formation of $(MeNBN(H)AlMe_2)_3$. ^1H NMR (C_6D_6): δ −0.62 (s, Al*Me*, 6H), 2.76 (s, N*Me*, 9H). $^{11}B\{^1H\}$ NMR (C_6D_6): δ 36.

A TGA scan for **7** under Ar purge showed a weight loss (40%) in the temperature range 100°−500 °C, and above that temperature there was very little weight loss until ∼1100 °C. On the basis of this observation, bulk pyrolysis of a sample of **7** (1.9 g) was accomplished in stages (50°−450 °C over 6 h, hold 2 h then 450°−1200 °C over 12 h) under a slow purge of NH_3 (2 L/min). Following cooling, a white powder (**8**) (0.96 g) was collected and characterized by IR, X-ray diffraction (XRD), energy-dispersive spectrometry (EDS), and transmission electron microscopy (TEM). Anal. Found: Al, 53.78; B, 1.96; N, 31.78.

Crystal Structure Determinations. Crystals were selected from preparative samples and mounted in glass capillaries under dry nitrogen. The crystals were mounted on a Siemens R3m/v automated diffractometer and determinations of crystal class, orientation matrix, and accurate unit cell parameters were performed in a standard fashion.[17] Data were collected in the ω scan mode using Mo Kα radiation, a scintillation counter, single crystal graphite monochromator, and pulse height analyzer. Selected crystal data are summarized in Table 1.

All calculations were performed on a SHELXTL structure determination system.[18,19] Structures were solved by direct methods and full matrix least-squares refinements were based on the function $\sum w(|F_o| - |F_c|)^2$. Some specific details for each structure determination are provided. $\mathbf{1}\cdot(Me_3B_3N_3Me_3)_{0.5}$. Colorless prism, 0.23 × 0.41 × 0.60 mm. The non-hydrogen atoms were refined anisotropically and the H-atoms were placed in idealized positions and refined (riding model) with $U_{iso} = 1.2U_{eqiv}$ of the parent atom. The molecule is accompanied by a half molecule of $(H_3CBNCH_3)_3$ in the lattice, and it resides on an inversion center such that the ring is disordered: each B/N atom of the ring has a 50% occupancy. **2**. Colorless chip, 0.21 × 0.38 × 0.58 mm. The non-hydrogen atoms were refined anisotropically, and the methyl H-atoms were placed in idealized positions and refined (riding model) with $U_{iso} = 1.25U_{eqiv}$ of the parent C-atom. The H-atoms on the N atoms were located in difference maps and allowed to vary in position with $U_{iso} = 1.25U_{eqiv}$ of the N-atom. **3**. Colorless prism, 0.16 × 0.25 × 0.53 mm. The non-hydrogen atoms were refined anisotropically and H-atoms were included in idealized positions and refined isotropically with $U_{iso} = 1.25U_{eqiv}$ of the parent atom. The methyl carbon atoms on Si1 are disordered over four positions each with one-fourth occupancy. **4**. Colorless block, 0.21 × 0.35 × 0.41 mm. All non-hydrogen atoms in the Al_2N_2 dimer unit were refined anisotropically. The H-atoms were included in idealized positions and refined (riding model) with $U_{iso} = 1.25U_{eqiv}$ of the parent atom. H1 on N1 was located and allowed to vary in position and U_{iso}. **6**. Colorless rectangular prism, 0.14 × 0.23 × 0.60 mm. All non-hydrogen atoms in the Al_2N_2 dimer unit were refined anisotropically. The H-atoms on C-atoms were placed in idealized positions and refined isotropically with $U_{iso} = 1.25U_{eqiv}$., and the H atoms on the bridging N atoms were located and allowed to vary in position with $U_{iso} = 1.25U_{eqiv}$ of the N-atom. The dimer molecule is accompanied by a molecule of $[Me_3N_3B_3(Me)_2(NH_2)]$ in the lattice that has B and N atoms of the ring positionally disordered with equal occupancy. The heavy atoms were refined isotropically, and the H atoms added in idealized positions (riding model).

Results and Discussion

The reactions of 1,3,4,5,6-pentamethyl-2-aminoborazine, $Me_3N_3B_3Me_2(NH_2)$ (**PMAB**), with $(Me_3Si)_3Al\cdot OEt_2$, Me_3Al, Et_3Al, and *i*-Bu_3Al were examined in hexane and toluene.

(17) Programs used for centering reflections, autoindexing, refinement of cell parameters and axial photographs are those described in: Sparks, R. A. *Nicolet P3*/*R3 Operations Manual*; Syntex Analytical Instruments: Cupertino, CA, 1978.

(18) The SHELXTL, package of programs for calculations and plots is described in: Sheldrick, G. M. *SHELXTL Users Manual, Revision 3*; Nicolet XRD Corp.: Cupertino, CA, 1981.

(19) SHELXTL uses scattering factors and anomalous dispersion terms taken from: *International Tables of X-Ray Crystallography*; Kynoch: Birmingham, England, 1968; Vol. *IV*.

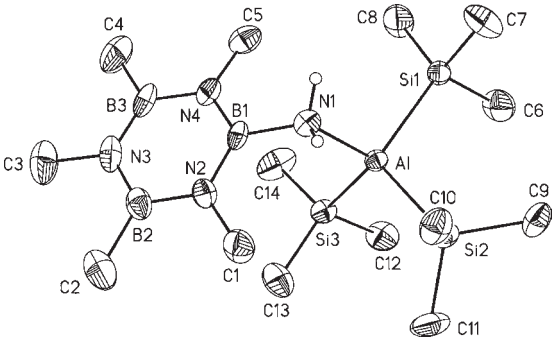

Figure 1. Molecular structure and atom numbering scheme for $\mathbf{1}\cdot(\mathbf{Me_3B_3N_3Me_3})_{0.5}$. The solvate molecule $Me_3B_3N_3Me_3$ is not shown.

Only $(Me_3Si)_3Al\cdot OEt_2$ produces a Lewis acid−base adduct, $(Me_3Si)_3Al\cdot$(**PMAB**) (**1**), that could be characterized, and the chemistry is summarized in eq 1. The product **1** is stable in hot (60 °C) hexane for hours, and it is isolated as a crystalline solid. The electron impact mass spectrum

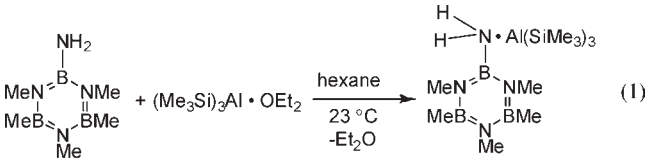

(1)

1

reveals a parent ion and fragment ions typical of an acid−base adduct. The ^1H, $^{11}B\{^1H\}$ and $^{13}C\{^1H\}$ NMR spectra were obtained and fully assigned.[21] It is noted that the coordination shifts for the donor ($\Delta\delta_D = \delta_{complex} - \delta_{PMAB}$) and acceptor ($\Delta\delta_A = \delta_{complex} - \delta_{TMS_3Al}$) fragments are small in both ^1H and $^{13}C\{^1H\}$ spectra. This includes $\Delta_D = -0.04$ ppm for the NH_2 protons and $\Delta_A = 0.04$ ppm for the Me_3Si protons. The $^{11}B\{^1H\}$ coordination shifts are slightly greater: $\Delta_{B4,6} = 1.4$ ppm and $\Delta_{B2} = 1.1$ ppm. Both ^{11}B coordination shifts are downfield consistent with electron withdrawal from the *exo*-NH_2 group upon interaction with the alane acceptor.

To confirm the structure of **1**, a single crystal X-ray diffraction analysis was completed. A view of the molecule is shown in Figure 1, and selected bond lengths are summarized in Table 2. Each molecule of **1** is accompanied by a half molecule of the borazine $(CH_3BNCH_3)_3$ that resides on a center of symmetry with B and N atoms positionally disordered. The adduct is monomeric with pseudo-tetrahedral aluminum and nitrogen atoms joined via an Al−N dative bond. The Al−N1 bond length, 2.078(7) Å is similar to bond lengths in $H_3Al\cdot NMe_3$, 2.063(8) Å,[22] $Me_3Al\cdot NMe_3$, 2.100(1) Å,[23] and

Table 2. Selected Bond Lengths (Å) and Bond Angles (deg) for $\mathbf{1}\cdot(\mathbf{Me_3B_3N_3Me_3})_{0.5}$, **2**, **3**, **4**, and $\mathbf{6}\cdot[\mathbf{Me_3N_3B_3(Me)_2(NH_2)}]_{0.5}$.

compound	bond lengths	bond angles	
		$\mathbf{1}\cdot(\mathbf{Me_3B_3N_3Me_3})_{0.5}$	
Al−N1	2.078(7)	N1−Al−Si1	107.6(2)
Al−Si1	2.471(3)	N1−Al−Si2	102.8(2)
Al−Si2	2.483(3)	N1−Al−Si3	109.2(2)
Al−Si3	2.471(3)	Si1−Al−Si2	110.4(1)
B1−N1	1.50(1)	Si2−Al−Si3	114.3(1)
B1−N2	1.41(1)	Si1−Al−Si3	111.9(1)
B1−N4	1.41(1)	Al−N1−B1	116.9(5)
B2−N2	1.42(1)	N1−B1−N2	119.6(7)
B2−N3	1.44(2)	N1−B1−N4	119.1(7)
B3−N3	1.43(1)	N2−B1−N4	121.2(7)
B3−N4	1.43(1)		
		2	
Al−N1	1.986(5)	N1−Al−N1′	87.4(2)
Al−N1′	1.982(4)	N1−Al−Si1	110.1(2)
Al···Al′	2.869(3)	N1−Al−Si2	118.6(2)
Al−Si1	2.482(3)	Si1−Al−Si2	107.7(1)
Al−Si2	2.479(2)	N1′−Al-Si1	121.9(2)
B1−N1	1.492(8)	N1′−Al-Si2	110.7(2)
B1−N2	1.424(8)	Al−N1−Al′	92.6(2)
B1−N4	1.396(8)	B1−N1−Al	125.7(3)
B2−N2	1.44(1)	B1−N1−Al′	133.8(4)
B2−N3	1.42(1)	N1−B1−N2	122.8(6)
B3−N3	1.40(1)	N2−B1−N4	118.6(6)
B3−N4	1.45(1)	N1−B1−N4	118.6(5)
		3	
Al1−N2	1.923(9)	N2−Al1−N3	91.3(4)
Al1−N3	1.91(1)	N2−Al1−N2′	90.2(6)
Al1−Si1	2.483(9)	N2−Al2−N3	89.6(5)
Al2−N1	1.91(1)	N1−Al2−N3	90.3(4)
Al2−N3	1.95(1)	N1−Al2−N2	89.4(5)
Al2−Si2	2.467(5)	N2−Al3−N2′	89.4(6)
Al3−N1	1.89(1)	N1−Al3−N2	90.5(4)
Al3−N2	1.94(1)		
Al3−Si3	2.45(1)		
Al1···Al2	2.722(5)		
Al1···Al3	2.734(7)		
Al2···Al2′	2.719(6)		
N2−Si4	1.728(9)		
N3−Si5	1.73(2)		
		4	
Al−N1	1.963(3)	N1−Al−N1′	87.1(2)
Al−N1′	1.974(4)	C1−Al−C2	113.3(2)
Al−C1	1.950(6)	N1−Al−C1	117.1(2)
Al−C2	1.956(4)	N1−Al−C2	109.9(2)
Al···Al′	2.854(3)	Al−N1−B1	131.6(3)
B1−N1	1.484(6)	Al−N1−Al′	92.9(2)
B1−N2	1.426(5)	B1−N1−Al′	125.7(3)
B1−N4	1.433(5)	N1−B1−N2	122.7(4)
B2−N2	1.433(6)	N1−B1−N4	119.1(3)
B2−N3	1.433(6)	N2−B1−N4	118.2(4)
B3−N3	1.423(6)		
B3−N4	1.443(6)		
		$\mathbf{6}\cdot[\mathbf{Me_3N_3B_3(Me)_2(NH_2)}]_{0.5}$	
Al−N1	1.986(6)	N1−Al−N1′	87.0(2)
Al−N1′	1.970(6)	C6−Al−C10	117.8(3)
Al−C6	1.975(7)	N1−Al−C6	114.4(3)
Al−C10	1.974(7)	N1−Al−C10	109.5(1)
Al···Al′	2.870(4)	C6−Al−N1′	108.5(3)
B1−N1	1.500(9)	C10−Al−N1′	115.9(3)
B1−N2	1.41(1)	Al−N1−B1	124.8(4)
B1−N4	1.44(1)	Al−N1−Al′	93.0(2)
B2−N2	1.444(9)	B1−N1−Al′	132.4(4)
B2−N3	1.43(1)	N1−B1−N2	122.3(6)
B3−N3	1.40(1)	N1−B1−N4	119.2(6)
B3−N4	1.443(1)	N2−B1−N4	118.6(6)

(20) Beachley, O. T.; Tessier-Youngs, C. *Inorg. Chem.* **1979**, *18*, 3188–3191.

(21) The NMR spectra for **1** can be compared with data for the acid and base fragment molecules $(Me_3Si)_3Al\cdot OEt_2$ ^1H NMR (C_6D_6): δ 0.24 (27 H, Si*Me*), 0.73 (6 H, OCH_2CH_3), 3.34 (4 H, OCH_2CH_3). $^{13}C\{^1H\}$ NMR (C_6D_6): δ 2.84 (Si*Me*), 13.19 (OCH_2CH_3), 69.63 (OCH_2CH_3). $Me_3N_3B_3Me_2(NH_2)$ ^1H NMR (C_6D_6): δ 0.47 (6 H, B-4, 6 *Me*), 1.93 (2 H, NH_2), 2.56 (6 H, N-1,3 *Me*), 2.77 (3 H, N-5 *Me*). $^{13}C\{^1H\}$ NMR (C_6D_6): δ-0.10 (B-4,6 Me), 31.75 (N-1,3 *Me*), 34.53 (N-5 *Me*). $^{11}B\{^1H\}$ NMR (C_6D_6): δ 26.2 (B-2), 36.3 (B-4,6).

(22) Almennigen, A.; Gundersen, G.; Haugen, T.; Haaland, A. *Acta Chem. Scand.* **1972**, *26*, 3928–3934.

(23) Anderson, G. A.; Almennigen, A.; Fargaard, F. R.; Haaland, A. *J. Chem. Soc., Chem. Commun.* **1971**, 480–481.

(24) Janik, J. F.; Duesler, E. N.; Paine, R. T. *J. Organomet. Chem.* **1997**, *539*, 19–25.

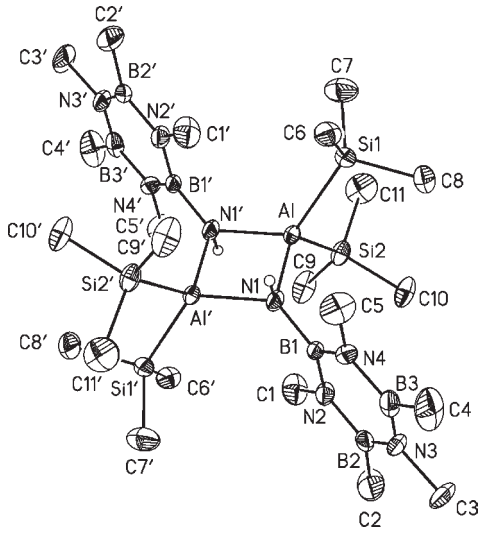

Figure 2. Molecular structure and atom numbering scheme for **2**. Molecular structures of **4** and **6** are isostructural with **2**.

$(Me_3Si)_3Al\cdot NMe_3$, 2.040(6) Å.[24] The average Al−Si bond length, 2.475(3) Å, is identical to the average value in $(Me_3Si)_3Al\cdot OEt_2$, 2.471(4) Å,[25] $(Me_3Si)_3Al\cdot TMEDA$, 2.472(3) Å[26] and $(Me_3Si)_3Al\cdot NMe_3$, 2.473(3) Å.[24] The *exo* B1−N1 bond length, 1.50(1) Å, as expected, falls in the covalent single bond range, and it is longer than the average B−N bond length in the borazine ring (1.42(1) Å). Further, the B1−N1 bond length is identical to the *exo* B−N bond lengths in the monoamino-borazine $[(HN)_3(HB)_2(BNH_2)]$,[27] 1.498(8) Å, and it is shorter than the N → B dative bond length in $H_3B\cdot NH_3$, 1.56(5) Å.[28] However, the B1−N1 bond length is longer than the average B−N bond length in $B(NMe_2)_3$,[29] 1.43(1) Å, and the *exo* B−N bond length in $(Me_2NBNH)_3$,[30] 1.429(8) Å. In these last examples, the shorter B−N bond lengths and planar nitrogen atom geometry indicate significant participation of B−N π overlap. The average borazine ring B−N bond length in **1** is similar to average B−N bond lengths in $(HBNH)_3$,[31] 1.436(2) Å, and in $(Me_2NBNH)_3$,[30] 1.433(8) Å.

The adduct **1** melts in the range 95−97 °C with evolution of Me_3SiH which was identified by IR spectroscopy. Similarly, the adduct decomposes by Me_3SiH evolution when refluxed in toluene, and a crystalline solid $[(Me_3Si)_2AlN(H)B_3Me_2N_3Me_3]_2$ (**2**) was isolated in high yield (85%). The chemistry is summarized in eq 2. The CHN analytical data for **2**, and also for several other of the compounds obtained here with the aluminum alkyls, are not in ideal agreement with the proposed composition.[32] However, the highest mass ion observed in an electron impact mass spectrum appears at *m*/*z* 661, and this corresponds to the mass of the dimer **2** minus one CH_3 group. The NMR spectra are consistent with the observation of Me_3SiH elimination and formation of a $(Me_3Si)_2AlN(H)B_3Me_2N_3Me_3$ molecular unit. Further, the NMR data for the isolated solid **2** indicate formation of a mixture of *cis* and *trans* isomers of a dimer $[(Me_3Si)_2AlN(H)B_3Me_2N_3Me_3]_2$.

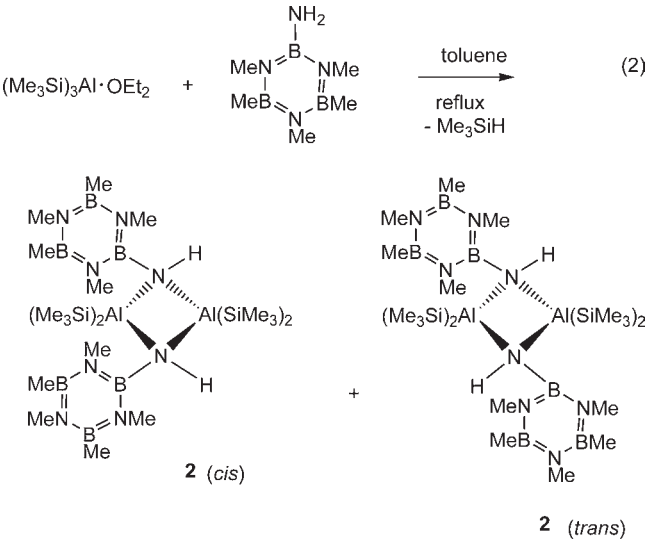

In C_6D_6 solution, the ^1H NMR peak intensities indicate a ratio *trans*/*cis* = 2.8:1. The ^1H and ^{13}C chemical shifts for each environment in **2** are similar to the related environment shifts in **1** except for the bridging amino group; the bridging amino protons in **2** appear as a broad singlet: *cis* δ 3.55 and *trans* δ 3.63. These are shifted significantly downfield relative to the shift for the terminal, coordinated NH_2 protons in **1**: δ 1.89. The ^{13}C resonance for the B4,6-Me groups in both the *cis* and *trans* isomers of **2** were not resolved.

A crystal structure determination for **2** confirms the formation of a dimer, and the molecule is present as the *trans* isomer in the solid state. A view of the molecule is shown in Figure 2, and selected bond distances are provided in Table 2. Attempts were made to sort through several batches of crystals of **2** in an effort to locate a different crystal morphology that might indicate the presence of the *cis* isomer, but this was unsuccessful. The Al and N atoms are four coordinate, and the Al_2N_2 ring is centrosymmetric with Al−N1 1.986(5) Å and Al−N1′ 1.982(4) Å, and internal ring bond angles N1−Al−N′ 87.4(2)° and Al−N−Al′ 92.6(2)°. The observed Al−N bond lengths are longer than those reported for several other amido alane dimers: $(Me_2AlNMe_2)_2$ 1.958(5) Å,[33] $[(Me_3Si)_2AlNH_2]_2$ avg. 1.955(2) Å,[11a] *trans* $[Me_2AlN(H)(1\text{-}Ad)]_2$ 1.968(2) Å,[10a] *trans* $[Me_2AlN(H)(i\text{-}Pr)]_2$ 1.959(5) Å.[34] The distance is more comparable with the Al−N bond lengths in $[Me_2AlN(SiHMe_2)_2]_2$ 1.992(3) Å[35] and $[(i\text{-}Bu)_2AlN(H)Bp]_2$ avg. 1.976(3) Å.[36] The long distance in **2** likely

(25) Rösch, L.; Altnau, G.; Kruger, C.; Tsay, Y. -H. *Z. Naturforsch.* **1983**, *38B*, 34–41.
(26) Goebel, D. W.; Hencher, J. L.; Oliver, J. P. *Organometallics* **1983**, *2*, 746–750.
(27) Harshbarger, W.; Lee, G. H.; Porter, R. F.; Bauer, S. H. *J. Am. Chem. Soc.* **1969**, *91*, 551–555.
(28) Hughes, E. W. *J. Am. Chem. Soc.* **1956**, *78*, 502–503.
(29) Clark, A. H.; Anderson, G. A. *J. Chem. Soc. Chem. Commun.* **1969**, 1082–1084.
(30) Hess, H.; Reiser, B. *Z. Anorg. Allg. Chem.* **1971**, *381*, 91–98.
(31) Harshbarger, W.; Lee, G.; Porter, R. F.; Bauer, S. H. *Inorg. Chem.* **1969**, *8*, 1683–1689.
(32) The descrepancies in CHN analytical data result from incomplete combustion of the samples as noted in analysis reports from commercial sources. This is likely due to formation of ceramic residues. Similar observations were made with analyses of $[(Me_3Si)_2AlNH_2]_2$.[11a]
(33) McLaughlin, G. M.; Sim, G. A.; Smith, J. D. *J. Chem. Soc., Dalton Trans.* **1972**, 2197–2203.
(34) Amirkhalili, S.; Hitchcock, P. B.; Jenkins, A. D.; Nyathi, J. Z.; Smith, J. D. *J. Chem. Soc., Dalton Trans.* **1981**, 377–380.
(35) Byers, J. J.; Pennington, W. T.; Robinson, G. H.; Hrncir, D. C. *Polyhedron* **1990**, *9*, 2205–2210.
(36) Byers, J. J.; Lee, B.; Pennington, W. T.; Robinson, G. H. *Polyhedron* **1992**, *11*, 967–972.

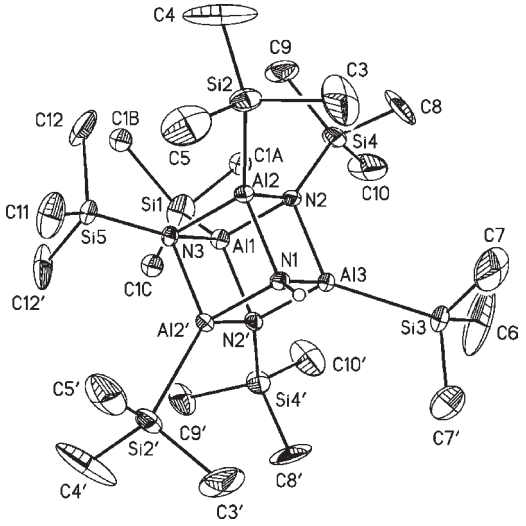

Figure 3. Molecular structure and atom numbering scheme for **3**.

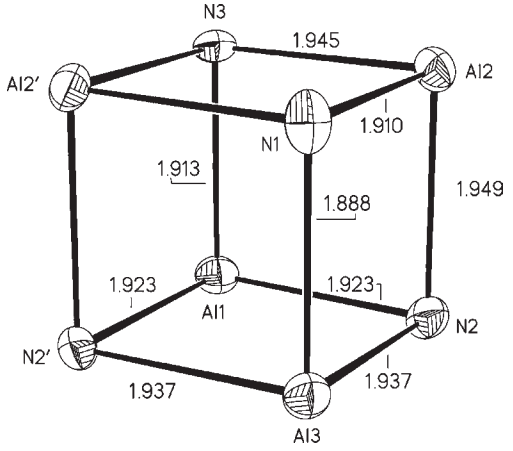

Figure 4. Selected Al_4N_4 cubane core bond lengths (Å) for **3**.

reflects the presence of sterically large groups on both the Al and the N atoms of the (Al_2N_2) ring. In response to minimizing the repulsions, the borazine rings are rotated so that they are perpendicular to the (Al_2N_2) plane. The Al−Si bond length (avg. 2.481(3) Å) is identical to that in **1**. The nonbonded Al···Al′ separation is 2.87(1) Å, and this is greater than the separation in the less congested dimer {$(Me_3Si)_2$-$AlNH_2]_2$, 2.838(1) Å.[11a]

In an attempt to drive the silane elimination chemistry further, toluene solutions of **2** were heated under vigorous reflux for several days. ^{1}H NMR spectra of the reaction mixture indicate that **2** is relatively stable under this condition, but slow formation of a minor soluble product is evidenced by new low intensity ^{1}H NMR resonances at δ 0.35 and 0.46. Eventually some insoluble material is also formed. Although sufficient amounts of the minor product for detailed spectroscopic characterization were not obtained, crystallization of the toluene soluble fraction produced crystal samples that contained small numbers of blocky, prismatic crystals notably different from crystals of **2**. Subsequent single crystal X-ray diffraction analysis revealed the formation of a compound with the unexpected composition [$(Me_3SiAl)_4(Me_3SiN)_3(NH)$], **3**. A view of the structure is shown in Figure 3, and selected bond lengths and bond angles are provided in Table 2. The structure of **3** consists of a cubane Al_4N_4 core similar in nature to several other imino alane condensation products. However, a unique feature appears here in that the cubane **3** is asymmetric. Each of the four Al-atom vertices is bonded to a single terminal Me_3Si group, but three of the four N-atom vertices are bonded to a terminal Me_3Si group while the fourth N-atom has a H-atom substituent. As shown in Figure 4, the N-atom substituent asymmetry is accompanied by asymmetry in the cubane bond lengths: Al−N bond lengths vary in the range 1.88(1)−1.95(1) (avg. 1.92 Å). Although the detailed mechanism for the formation of **3** remains undefined, the structure suggests that B−N bond cleavage in **2** occurs, and the elimination of a borazine, perhaps $HB_3(Me)_2N_3Me_3$, occurs with silyl migration from aluminum to nitrogen. Under the refluxing toluene condition, this is apparently not a facile reaction.

It is worth noting that the formation of **1** and the somewhat forcing conditions needed to produce **2** are in contrast to the ease of reaction between $(Me_3Si)_3Al\cdot OEt_2$ and NH_3.[11a,b] In that system, no adduct was isolated. The onset of Me_3SiH elimination was well below 0 °C in hydrocarbon solution leading to formation of the dimer $[(Me_3Si)_2AlNH_2]_2$. With this comparison in mind, the reactions of **PMAB** with the aluminum trialkyls Me_3Al, Et_3Al, and *i*-Bu_3Al were examined. In no case was there evidence for the formation of an adduct. With Me_3Al and Et_3Al, CH_4 and C_2H_6 evolution was evident at 23 °C as soon as the reagents were mixed. The reaction with *i*-Bu_3Al was slower at 23 °C, and it accelerated in refluxing toluene solution. The resulting products $[Me_2AlN(H)B_3(Me)_2N_3Me_3]_2$ **4**, $[Et_2AlN(H)B_3(Me)_2$-$N_3Me_3]_2$ **5** and $[i\text{-}Bu_2AlN(H)B_3(Me)_2N_3Me_3]_2$ **6** were isolated as crystalline solids in good yield. As found with **2**, the CHN analyses are not entirely satisfactory as small amounts of residue form in the combustion analyses.[32] The NMR spectra for **4**−**6** are similar to those for **2** with each showing mixtures of *trans*/*cis* isomers in benzene with ratios 1.6/1, 1.1/1, and 1/2 at 23 °C.

X-ray structure determinations for **4** and **6** were completed, and both molecules are isostructural with **2**. Selected bond lengths and bond angles are presented in Table 2. Both molecules in the solid state exist in a planar *trans* configuration with geometric parameters similar to **2**: **4**, Al−N1 1.963(3) Å and Al′−N1′ 1.974(4) Å, Al···Al′ 2.854(3) Å; **6**, Al−N1 1.986(6) Å, Al−N′ 1.970(6) Å, Al···Al′ 2.870(4) Å.

Polymeric/Ceramic Conversion

On the basis of our previous utilization of several poly(borazinylamine) pre-ceramic polymers to prepare metal nitride/boron nitride composites, we examined here the reaction of Me_3Al with 1,3,5-*N*-trimethyl-2,4,6-*B*-triamino borazine **7** in a 3:1 mol ratio in toluene at 23 °C (45 h) and under reflux (1 h). The mixture evolved methane which was detected by IR spectroscopy, and following removal of the solvent, a glassy solid **8** was obtained that remained soluble in toluene and benzene. An idealized representation of the chemistry is shown in eq 3. The molecular representation of **8** is probably not fully accurate; however, the ready solubility of **8** in benzene and toluene suggests that cross-linking, under the synthesis conditions used, is probably not extensive. ^{1}H NMR for **8** in C_6D_6 shows a resonance at δ −0.62 that is

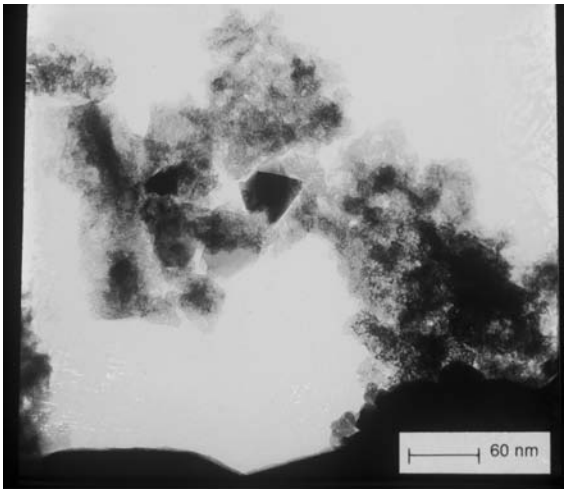

Figure 5. Transmission electron micrograph (TEM) for AlN/BN composite powder.

assigned to Al*Me* protons and a second resonance at δ 2.76 is assigned to N*Me*.

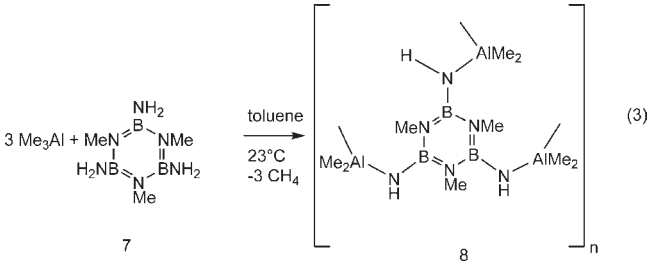

These appear in an approximate 2:1 area ratio. The resonance for the N*H* protons was not located. The $^{11}B\{^1H\}$ NMR spectrum contains a single resonance at δ 36.

A TGA scan for **8** shows a significant weight loss (~25 wt %) between ~100 and 150 °C and a more gradual weight loss (~15%) between 150 and 500 °C. From there to ~1100 °C the weight is constant followed by a small weight loss (~10%) between 1100 and 1400 °C. The weight loss in the 100°−150 °C region is largely due to methane evolution; however, identification of the off-gases formed at higher temperatures was not made. This suggests that the early stage of pyrolysis of this molecular precursor system probably is dominated by cross-linking and iminoalane formation followed most likely by borazine ring-opening and condensation processes. Using the TGA data to develop a heating program, **8** was heated under a slow NH_3 purge from 100°−450 °C (6 h) and 450°−1200 °C (12 h). From this, a white powder **9** was obtained in 51% yield. Partial elemental analysis for a sample of **9** showed Al 53.78, B 1.96, and N 31.78% (total 87.52%; partial empirical composition $Al_{1.0}$ $B_{0.1}$ $N_{1.1}$). The remainder of the composition is composed of C, H, and O whose amounts were not reliably assessed. Powder XRD scans for the product show the production of well crystallized AlN with sharp lines (d = 2.693, 2.484, 2.362, 1.826, 1.553, 1.411, 1.345, 1.319, 1.290) that are almost identical to values for authentic samples of AlN (hexagonal wurtzite):[37] d = 2.695 (100), 2.490 (002), 2.371 (101), 1.829 (102), 1.556 (110), 1.413 (103), 1.348 (200), 1.319 (112), 1.301 (201). The XRD scans do not show the formation of crystalline BN which suggests that the BN formed is amorphous or turbostratic. A similar suppression of BN crystallization was seen in the formation of TiN/BN composites.[38] A TEM (Figure 5) for the pyrolysis product shows the formation of nanosized crystallites of AlN dispersed in a matrix of BN. The edges of the crystallites of AlN show no clear evidence for growth of BN on the AlN surface.

Conclusion

The reactions of $(Me_3Si)_3Al\cdot OEt_2$, Me_3Al, Et_3Al, and i-Bu_3Al with the primary borazinyl amine, $Me_3N_3B_3Me_2(NH_2)$ **PMAB**, have been explored and only in the combination of $(Me_3Si)_3Al\cdot OEt_2$ and **PMAB** is evidence for the formation of an acid−base adduct detected. Consistent with the supposition that formation of acid−base adducts retard intramolecular elimination chemistry, it is found that this combination is less facile in silane elimination than the combinations of Me_3Al, Et_3Al, and i-Bu_3Al with **PMAB** that display rapid alkane elimination. In each case, the primary elimination reaction product is the respective dimeric amino alane, $[R_2AlN(H)\mathbf{PMAB}]_2$, and each is formed in organic solvent as a mixture of *cis* and *trans* isomers. The dimers are relatively stable for extended periods in refluxing toluene; however, $[(Me_3Si)_2AlN(H)\mathbf{PMAB}]_2$ is found to slowly produce a cubane-like iminoalane, $[(Me_3SiAl)_4(Me_3SiN)_3(NH)]$, **3**. The mechanism for the formation of **3** was not deduced. However, it appears that N−B bond breaking with elimination of the borazine $Me_3N_3B_3(H)Me_2$ accompanied by terminal silyl migration to three of the four imino N-atoms provides a competing pathway for elimination that is apparently favored over simple Me_3SiH elimination. The appearance of a process that involves loss of a volatile borazine may be responsible for the reduced boron content in the high temperature pyrolysis product obtained by heating **8** at 1200 °C.

Acknowledgment. Financial support from the National Science Foundation (CHE-9983205) (RTP) enabled this study.

Supporting Information Available: X-ray crystallographic data including data collection and structure solution details and tables of atom position coordinates, thermal factors, bond distances and bond angles. This material is available free of charge via the Internet at http://pubs.acs.org. The crystallographic data have also been deposited at the Cambridge Crystallographic Data Centre under the following deposition numbers: 611276, 611278−611281.

(37) Powder Diffraction File Card No. 25−1133, JCPDS, International Center for Powder Diffraction Data, Swarthmore, PA, **1975**.
(38) Paine, R. T.; Janik, J. F.; Fan, M. *Polyhedron* **1984**, *13*, 1225–1232.